Available online at www.sciencedirect.com

ScienceDirect

Ceramics International 40 (2014) 1221–1224

CERAMICS INTERNATIONAL

www.elsevier.com/locate/ceramint

Short communication

Fabrication of *c*-axis-oriented apatite-type polycrystalline $La_{10}Si_6O_{27}$ ceramic and its anisotropic oxide ionic conductivity

Susumu Nakayama[a,*], Yoshikatsu Higuchi[b], Masayuki Sugawara[b], Atsushi Makiya[c], Keizo Uematsu[c], Masatomi Sakamoto[d]

[a]*Department of Applied Chemistry and Biotechnology, Niihama National College of Technology, 7-1 Yagumo-cho, Niihama-shi 792-8580, Japan*

[b]*Honda Research and Development Co., Ltd., Wako-shi 351-0193, Japan*

[c]*Department of Materials Science and Technology, Nagaoka University of Technology, Nagaoka-shi, 940-2188, Japan*

[d]*Material and Biological Chemistry, Graduate School of Science and Engineering, Yamagata University, Yamagata-shi 990-8560, Japan*

Received 9 April 2013; received in revised form 22 May 2013; accepted 22 May 2013

Available online 13 June 2013

Abstract

The *c*-axis-oriented apatite-type lanthanum silicate, $La_{10}Si_6O_{27}$, ceramic was successfully fabricated by an application of a high magnetic field followed by a sintering process. Degree of an orientation in the $La_{10}Si_6O_{27}$ ceramic sintered at 1700 °C was 48.1% along (00*l*) on the Lotgering scale. Conductivity of the *c*-axis-oriented $La_{10}Si_6O_{27}$ ceramic is about 0.5 orders of magnitude higher than that of the non-oriented $La_{10}Si_6O_{27}$ ceramic. The higher conductivity is caused by an orientation of oxide ions in the grains composing the ceramic, which are located along the *c*-axis and responsible for the ionic conduction.

Keywords: Apatite-type structure; Oxide ionic conductor; Lanthanum silicate; X-ray method

1. Introduction

We reported a series of apatite-type rare earth silicates, $RE_xSi_6O_{1.5x+12}$ (x=8–11) including $RE_{10}Si_6O_{27}$ (RE=La–Dy), as a new type oxide ionic conductor [1–4]. Among these, lanthanum silicates (RE=La) showed high conductivities in the temperature region below 600 °C, suggesting that the lanthanum silicates are promising candidates for an intermediate temperature solid oxide fuel cell (IT-SOFC) as well as scandia-stabilized zirconia and $LaGaO_3$-based perovskite-type oxide [4]. Besides the above reports, several groups have also reported the electrical conductivity of lanthanum silicate with apatite-type structure [5–11]. However, these reports are limited to studies on the conductivity of polycrystalline lanthanum silicates. Since 1999, the anisotropy in oxide ionic conductivities of the rare earth silicate single crystals, $RE_{9.33}(SiO_4)_6O_2$ (RE=La, Pr, Nd and Sm), has been reported, and it has been found that the conductivity component parallel to the *c*-axis is about one order of magnitude higher than that of the perpendicular component [12–17]. The conduction mechanism of $RE_{9.33}(SiO_4)_6O_2$ can be understood from a structural analysis which proposed a hexagonal apatite structure ($P6_3/m$ space group). As shown in Fig. 1, oxide ions responsible for the conduction are located at the 2a site along the *c*-axis and are surrounded by rare earth ions of the 6 h site, indicating that the parallel migration of oxide ions to the *c*-axis will be much easier than the perpendicular migration. These observation and structural analysis tell that the preparation of the apatite-type $RE_{9.33}(SiO_4)_6O_2$ ceramics consisting of the *c*-axis-oriented grains leads to the improvement of conductivity. For the grain orientation, application of the magnetic field has been well known as one of the effective methods [18–23]. In this work, we report the preparation of the *c*-axis-oriented apatite-type polycrystalline lanthanum silicate ceramic, $La_{10}Si_6O_{27}$, under a high magnetic field and its oxide ionic conductivity.

*Corresponding author. Tel.: +81 897 377786.

E-mail address: nakayama@chem.niihama-nct.ac.jp (S. Nakayama).

0272-8842/$ - see front matter © 2013 Elsevier Ltd and Techna Group S.r.l. All rights reserved.

http://dx.doi.org/10.1016/j.ceramint.2013.05.136

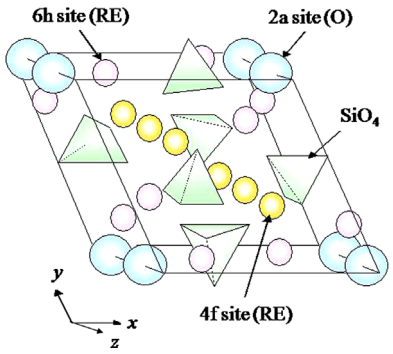

Fig. 1. Apatite structure proposed for $RE_{9.33}(SiO_4)_6O_2$ (RE=La–Dy).

2. Experimental

For the preparation of the $La_{10}Si_6O_{27}$ powder, La_2O_3 (99.9%–purity) and SiO_2 (99.9%–purity) were mixed in the desired ratios in ethanol by a planetary ball-mill using Y_2O_3-stabilized zirconia balls and plastic pot. The mixture was ball-milled for 5 h, dried and calcined in an alumina crucible in air at 1400 °C for 2 h. The resultant powder was further ball-milled into a fine powder. The powder was placed in a planetary ball mill with distilled water as a dispersant and zirconia balls, and then the mixture was well-mixed for 10 min to prepare a slurry with the solids loading of 20 vol%. After passing through a mesh with a 60 μm opening, the slurry was poured into a mold made of TEFLON. The mold was placed in a super-conducting magnet (TM-10VH10, Toshiba, Japan), and a magnetic field of 10 T was applied in the direction parallel to the mold at room temperature for more than overnight which was necessary to dry the slurry. The dried compact was sintered at 1700 °C for 2 h. For comparison, another compact was also prepared by a similar method except for the application of a magnetic field and sintered at 1700 °C for 2 h. Powder X-ray diffraction (XRD) patterns were recorded on Rigaku RINT 2100 with CuKα radiation (λ=0.15418 nm), in order to confirm the formation of an apatite structure. The XRD measurements were also carried out to evaluate the orientation of grains in the sintered ceramics using the Lotgering method [24]. Grain morphology of calcined powder and fracture surface of sintered ceramics were observed with a Scanning Electron Microscope (SEM, Hitachi TM-1000). The diameter and thickness of the samples manufactured for the conductivity measurement were 5 mm and 1 mm, respectively. After both sides of the samples were coated with Pt paste, the disc was baked at 950 °C. Conductivities were measured in the temperature range of 400–800 °C and in the frequency range of 100 Hz–10 MHz by an HP4194A impedance analyzer.

3. Results and discussion

Fig. 2 shows SEM photograph of the $La_{10}Si_6O_{27}$ powder calcined at 1400 °C. The particles are nearly angular in shape and their sizes vary from 0.1 to 1.0 μm. No agglomerates of the particles are observed. Fig. 3 shows SEM photographs of

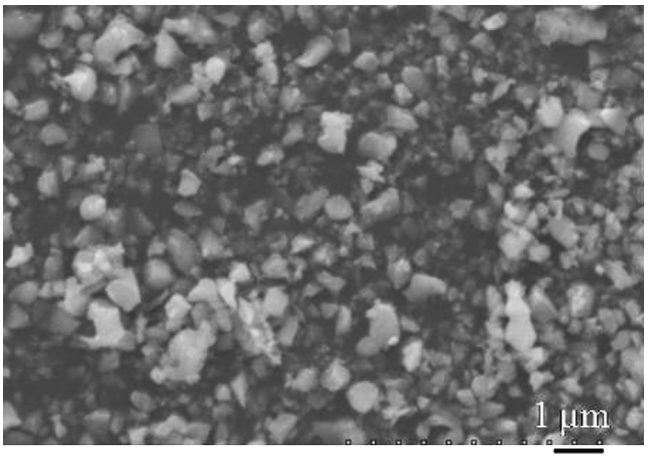

Fig. 2. SEM photograph of $La_{10}Si_6O_{27}$ powder prepared by calcining at 1400 °C.

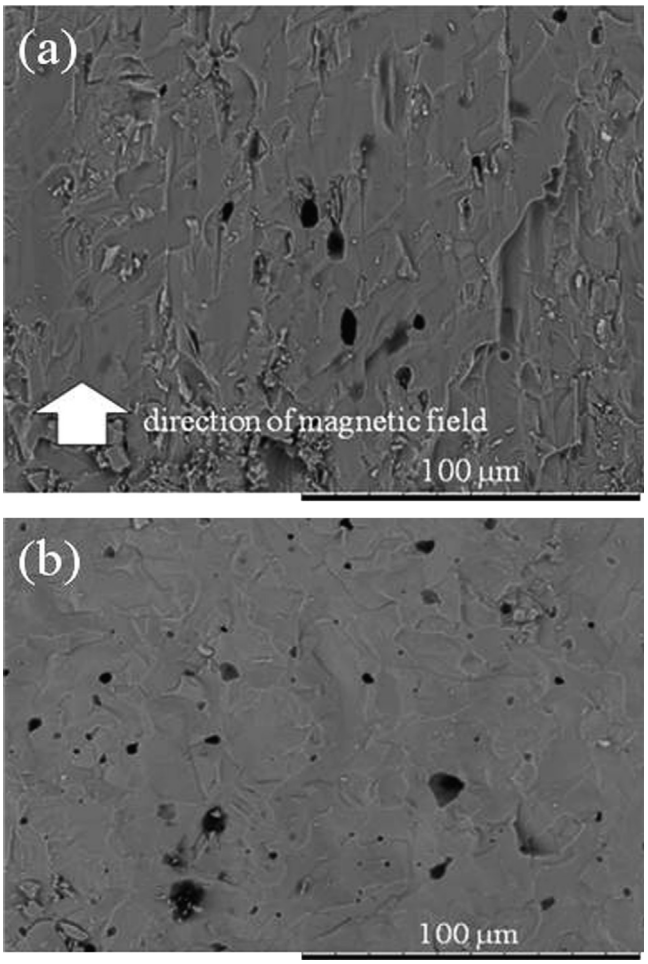

Fig. 3. SEM photographs of fracture surfaces of (a) the oriented ceramic prepared after applying magnetic field and (b) the non-oriented ceramic prepared without magnetic field.

fracture surface of the specimen sintered at 1700 °C after applying magnetic field (called the oriented ceramic, hereafter) and that of the specimen sintered at the same temperature without applying magnetic field (called the non-oriented ceramic, hereafter). As can be seen from Fig. 3(a), each grain

in the oriented ceramic is forced to be oriented in the direction of applied magnetic field. This is clearly distinguished from the randomly oriented grains observed in the SEM image for the non-oriented ceramic (see Fig. 3(b)). In spite of such apparent difference between these two specimens, almost the same densities were determined for the oriented and non-oriented ceramics (5.41 g cm^{-3} and 5.37 g cm^{-3}, respectively).

Fig. 4 shows the X-ray diffraction patterns for the oriented and non-oriented ceramics. The X-ray was contrived to be incident onto the surface perpendicular to the direction of the applied magnetic field for the oriented ceramic and onto the surface perpendicular to gravity for the non-oriented one (see the respective insets in Fig. 4). As can be seen in Fig. 4(a), the oriented ceramic gives two strong peaks due to diffraction from the (002) and (004) planes. The (102) peak observed at 27.5° is also rather strong, whereas peak due to diffraction from the (211) plane are weak. This may be reasonably explained as follows: the inter-planar angle between the basal (00*l*) and (102) planes is estimated to be 47.1°, and that between the (00*l*) and (211) planes is estimated to be 72.6° for the hexagonal unit cell with $a=0.98$ nm and $c=0.72$ nm. This means that the (102) plane is parallel to the *c*-plane compared with the (211) plane, leading to the relatively intense (102) peak. On the other hand, in the non-oriented ceramic (Fig. 4(b)), diffractions from the (210), (211), (222), (213), etc. were also strongly observed, indicating that the grains are randomly oriented. The *a*-and *c*-lattice parameters of the non-oriented ceramic were 0.975 nm and 0.721 nm, respectively. These results show that in the oriented ceramic, *c*-planes of the grains are rather perpendicular to the direction of the applied magnetic field. Degree of the orientation, *f*, can be calculated according to the following Lotgering expression (1) [24].

$$f = \frac{\rho - \rho_0}{1 - \rho_0} \tag{1}$$

Here, ρ_0 is the value for the non-oriented ceramic and can be determined from Fig. 4(b) using the Eq. (2), in which $\Sigma I_0(hkl)$ and $\Sigma I_0(00l)$ are the total intensity obtained adding the intensity of all peaks observed in the range of $20° < 2\theta < 60°$ and the sum of the (002) and (004) peak intensity, respectively.

$$\rho_0 = \frac{\Sigma I_0(00l)}{\Sigma I_0(hkl)} \tag{2}$$

The ρ-value in Eq. (1) can be determined from Fig. 4(a) using Eq. (3) $\Sigma I(hkl)$ and $\Sigma I(00l)$, which correspond to $\Sigma I_0(hkl)$ and $\Sigma I_0(00l)$ for the non-oriented ceramic, respectively, stand for the values for the oriented ceramic.

$$\rho = \frac{\Sigma I(00l)}{\Sigma I(hkl)} \tag{3}$$

Values of ρ_0 and ρ were estimated to be 0.057 and 0.452 from Fig. 4(b) and (a), respectively. By substituting these values for ρ_0 and ρ in Eq. (1), respectively, 0.419 (41.9%) was obtained as a degree of orientation for the present oriented $La_{10}Si_6O_{27}$ ceramic.

Conductivities of the oriented and non-oriented ceramics were determined applying the complex plane impedance analysis, by setting up the Pt electrodes as described in Experimental section (see the inset in Fig. 5). The complex plane impedance plots revealed that, at the lower temperatures (< 350 °C), the low-frequency plots are represented by a spike and the high-frequency plots by a semicircle which passes through the origin. When the temperature was increased (> 400 °C), the semicircle probably due to the electrolyte itself diminished and only a spike probably due to the electrolyte-electrode behavior became observed. From these results, the conductivity was determined by extrapolation to zero reactance of the complex impedance plot. These conductivity data were parameterized by the Arrhenius Eq. (4),

$$\sigma T = \sigma_0 \exp\left(\frac{-E}{kT}\right) \tag{4}$$

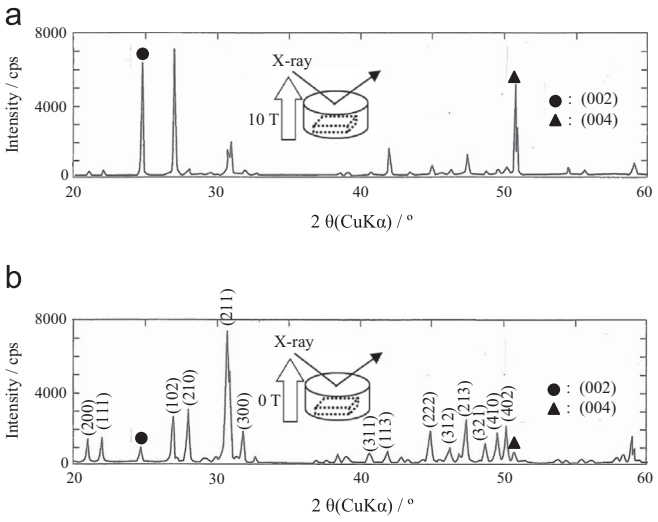

Fig. 4. X-ray diffraction patterns of (a) the oriented ceramic and (b) the non-oriented ceramic. Directions of the incident X-ray and the magnetic field are shown in the insets. (a) $La_{10}Si_6O_{27}$:10 T and (b) $La_{10}Si_6O_{27}$:0 T.

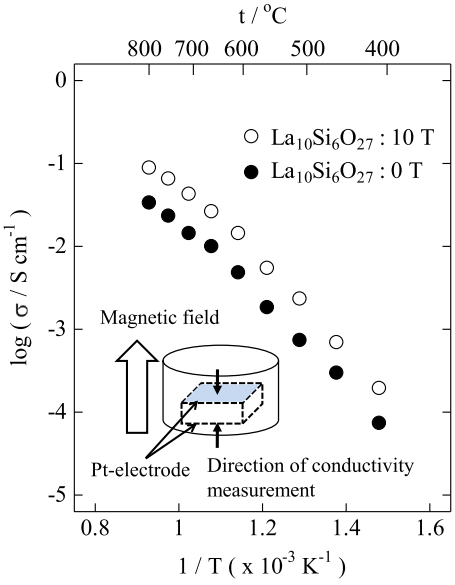

Fig. 5. Arrhenius plots of conductivities of the oriented ceramic and (b) the non-oriented ceramic. Conductivities of the oriented ceramic were measured in the direction of magnetic field as illustrated in the inset.

where σ, σ_0, E, k and T are the conductivity, pre-exponential factor, activation energy, Boltzmann constant and absolute temperature, respectively. Arrhenius plots of the oriented and non-oriented ceramics are shown in Fig. 5. At a given temperature, σ-value of the oriented ceramic is higher by about 0.5 orders of magnitude compared to that of the non-oriented ceramic. However, activation energies for the two ceramics are almost equal, suggesting that the conduction mechanism is not different from each other. Such anisotropy in conductivity was realized by the *c*-axis-orientation of each grain in the ceramic, as was visually confirmed from SEM photograph of Fig. 3(a).

4. Conclusion

The *c*-axis-oriented apatite-type lanthanum silicate ceramic, $La_{10}Si_6O_{27}$, has been prepared under a high magnetic field. The *c*-axes of the $La_{10}Si_6O_{27}$ grains are oriented parallel to the applied magnetic field. Using the Lotgering method, degree of the orientation (*f*) along (00*l*) was determined to be 48.1%. At a given temperature, its conductivity was higher by about 0.5 orders of magnitude than that of the non-oriented ceramic.

References

[1] S. Nakayama, H. Aono, Y. Sadaoka, Ionic conductivity of $Ln_{10}(SiO_4)_6O_3$ (Ln=La, Nd, Sm, Gd and Dy), Chemistry Letters 24 (1995) 431–432.

[2] S. Nakayama, T. Kageyama, H. Aono, Y. Sadaoka, Ionic conductivity of lanthanoid silicates, $Ln_{10}(SiO_4)_6O_3$ (Ln=La, Nd, Sm, Gd, Dy, Y, Ho, Er and Yb), Journal of Materials Chemistry 5 (1995) 1801–1805.

[3] S. Nakayama, M. Sakamoto, Electrical properties of new type high oxide ionic conductor $RE_{10}Si_6O_{27}$ (RE=La, Pr, Nd, Sm, Gd, Dy), Journal of the European Ceramic Society 18 (1998) 1413–1418.

[4] Y. Higuchi, M. Sugawara, K. Onishi, M. Sakamoto, S. Nakayama, Oxide ionic conductivities of apatite-type lanthanum silicates and germanates and their possibilities as an electrolyte of lower temperature operating SOFC, Ceramics International 36 (2010) 955–959.

[5] J.E.H. Sansom, D. Richings, P.R. Slater, A powder neutron diffraction study of the oxide-ion-conducting apatite-type phases, $La_{9.33}Si_6O_{26}$ and $La_8Sr_2Si_6O_{26}$, Solid State Ionics 139 (2001) 205–210.

[6] E.J. Abram E J, D.C. Sinclair, A.R. West, A novel enhancement of ionic conductivity in the cation-deficient apatite $La_{9.33}(SiO_4)_6O_2$, Journal of Materials Chemistry 11 (2001) 1978–1979.

[7] J.R. Tolchard, M.S. Islam, P.R. Slater, Defect chemistry and oxygen ion migration in the apatite-type materials $La_{9.33}(SiO_4)_6O_2$ and $La_8Sr_2Si_6O_{26}$, Journal of Materials Chemistry 16 (2003) 1956–1961.

[8] H. Yoshioka, S. Tanase, Magnesium doped lanthanum silicate with apatite-type structure as an electrolyte for intermediate temperature solid oxide fuel cells, Solid State Ionics 176 (2005) 2395–2398.

[9] T. Iwata, E. Bechade, K. Fukuoka, O. Masson, I. Julien, E. Champion, P. Thomas, Lantanum- and oxygen-deficient strauctures of oxide-ion conducting apatite-type silicates, Journal of the American Ceramic Society 91 (2008) 3714–3720.

[10] P.J. Panteix, I. Julien, P. Abelard, D. Bernache-Assollant, Influence of porosity on the electrical properties of $La_{9.33}(SiO_4)_6O_2$ oxyapatite, Ceramics International 34 (2008) 1579–1586.

[11] H. Yoshioka, Y. Nojiri, S. Tanase, Ionic conductivity and fuel cell properties of apatite-type lanthanum silicates doped with Mg and containing excess oxide ions, Solid State Ionics 179 (2008) 2165–2169.

[12] S. Nakayama, M. Sakamoto, M. Higuchi, K. Kodaira, M. Sato, S. Kakita, T. Suzuki, K. Itoh, Oxide ionic conductivity of apatite type $Nd_{9.33}(SiO_4)_6O_2$ single crystal, Journal of the European Ceramic Society 19 (1999) 507–510.

[13] S. Nakayama, M. Higuchi, Electrical properites of apatite type oxide ionic conductors $RE_{9.33}(SiO_4)_6O_2$ (RE=Pr, Nd and Sm) single crystals, Journal of Materials Science Letters 20 (2001) 913–915.

[14] M. Higuchi, Y. Masubuchi, S. Nakayama, S. Kikkawa, K. Kodaira, Single crystal growth and oxide ion conductivity of apatite-type rare-earth silicates, Solid State Ionics 174 (2004) 73–80.

[15] Y. Masubuchi, H. Higuchi, T. Takeda, S. Kikkawa, Oxide ion conduction mechanism in $RE_{9.33}(SiO_4)_6O_2$ and $Sr_2RE_8(SiO_4)_6O_2$ (RE=La, Nd) from neutron powder diffraction, Solid State Ionics 177 (2006) 263–268.

[16] K. Fukuda, T. Asaka, R. Hamaguchi, T. Suzuki, H. Oka, A. Berghout, E. Béchade, O. Masson, I. Julien, E. Champion, P. Thomas, Oxide-ion conductivity of highly *c*-axis-oriented apatite-type lanthanum silicate polycrystal formed by reactive diffusion between La_2SiO_5 and $La_2Si_2O_7$, Chemistry of Materials 23 (2011) 5474–5483.

[17] S. Nakayama, A. Ikesue, Y. Higuchi, M. Sugawara, M. Sakamoto, Growth of single-crystals of apatite-type oxide ionic conductor from sintered ceramics by a seeding method, Journal of the European Ceramic Society 33 (2013) 207–210.

[18] T.S. Suzuki, Y. Sakka, K. Kitazawa, Preferred orientation of the texture in the SiC whisker-dispersed Al_2O_3 ceramics by slip casting in a high magnetic field, Journal of the Ceramic Society of Japan 109 (2001) 886–890.

[19] T.S. Suzuki, Y. Sakka, K. Kitazawa, Orientation amplification of alumina by colloidal filtration in a strong magnetic field and sintering, Advanced Engineering Materials 3 (2001) 44–46.

[20] T.S. Suzuki, Y. Sakka, Control of texture in ZnO by slip casting in a strong magnetic field and heating, Chemistry Letters 31 (2002) 1204–1205.

[21] A. Makiya, D. Kusano, S. Tanaka, N. Uchida, K. Uematsu, T. Kimura, K. Kitazawa, Y. Doshida, Particle oriented bismuth titanate ceramics made in high magnetic field, Journal of the Ceramic Society of Japan 111 (2003) 702–704.

[22] H. Yi, X. Mao, G. Zhou, S. Chen, X. Zou, S. Wang, S. Shimai, Crystal plane evolution of grain oriented alumina ceramics with high transparency, Ceramics International 38 (2012) 5557–5561.

[23] L. Zhang, J. Vleugels, L. Darchuk, O.V. Biest, Magnetic field oriented tetragonal zirconia with anisotropic toughness, Journal of the European Ceramic Society 31 (2011) 1405–1412.

[24] F.K. Lotgering, Topotactical reaction with ferromagnetic oxides having hexagonal crystal, Journal of Inorganic and Nuclear Chemistry 9 (1959) 113–123.